ACS OMEGA

Article

Cite This: ACS Omega 2018, 3, 11608−11616

http://pubs.acs.org/journal/acsodf

Phenylene-Bridged OSSO-Type Titanium Complexes in the Polymerization of Ethylene and Propylene

Rosita Lapenta,[†] Antonio Buonerba,[†,‡] Ermanno Luciano,[†] Francesco Della Monica,[†] Assunta De Nisi,[§] Magda Monari,[§] Alfonso Grassi,[†,‡] Carmine Capacchione,[†,‡] and Stefano Milione*[,†,‡]

[†]Department of Chemistry and Biology, University of Salerno, via Giovanni Paolo II, 132, Fisciano I-84084, Salerno, Italy

[‡]Interuniversity Consortium Chemical Reactivity and Catalysis (CIRCC), via Celso Ulpiani 27, 70126 Bari, Italy

[§]Dipartimento di Chimica G. Ciamician, Alma Mater Studiorum, Università di Bologna, via Selmi 2, Bologna I-40126, Italy

Supporting Information

ABSTRACT: The dichloro titanium complexes $(OSSO_{tBu})TiCl_2$ (**1**) and $(OSSO_{Cum})TiCl_2$ (**2**) bearing *o*-phenylene-bridged OSSO-type ligands [$OSSO_{tBu}$-H = 6,6′-((1,2-phenylenebis(sulfanediyl))bis(methylene))bis(2,4-di-*tert*-butyphenol) and $OSSO_{Cum}$-H = 6,6′-((1,2-phenylenebis(sulfanediyl))bis(methylene))bis(2,4-bis(2-phenylpropan-2-yl)phenol)] were prepared and characterized. The X-ray structure of **1** revealed that Ti atom has an octahedral coordination geometry with an *fac*−*fac* wrapping of the [OSSO] ligand. In solution at 25 °C, **1** mainly retains the C_2 symmetric structure, whereas **2** shows an equilibrium between C_2- and C_1-symmetric stereoisomers. Activation of **2** with $(Ph_3C)[B(C_6F_5)_4]$ led to a highly active catalytic system with an activity of 238 $kg_{PE}{\cdot}mol_{cat}^{-1}{\cdot}bar^{-1}{\cdot}h^{-1}$; linear polyethylene with a T_m of 122 °C and M_w of 107 kDa were obtained under these conditions. Catalyst **1** displayed the moderate activity of 59 $kg_{PE}{\cdot}mol_{cat}^{-1}{\cdot}bar^{-1}{\cdot}h^{-1}$. Gel permeation chromatography analysis revealed the formation of high-molecular-weight polyethylenes with very large distributions of the molecular weights, indicating a low control of the polymerization process, probably becaue of the presence of different active species in solution. Density functional theory investigation provides a rational for the relative high-molecular-weight polymers obtained with these complexes. The precatalyst **2** was also active in propylene polymerization producing atactic oligomers terminated with unsaturated end groups.

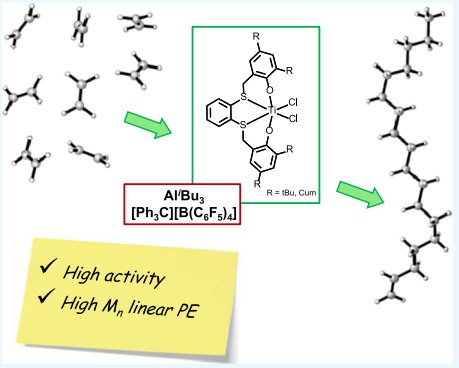

INTRODUCTION

The last decades have witnessed the development of new nonmetallocene early-transition metal complexes as catalyst precursors for olefin polymerization.[1] Among these, group 4 complexes of polydentate ligands, based on a bis(phenolate) framework with additional donors, are particularly acknowledged.[2] Indeed, Fujita[3] and Coates[4] reported on bis(phenoxy-imine) group 4 complexes that are very active in the ethylene polymerization and produce syndiotactic polypropylene under living conditions. Later on, Kol et al. developed a zirconium complex coordinated by a diamine bis(phenolate) [ONNO]-type ligand that is able to promote the living polymerization of 1-hexene with high isospecificity.[5] Since then, several group 4 metal complexes featuring [ONNO]-,[6] [OSSO]-,[7] [OOOO]-,[8] and [OPPO]-type[9] tetradentate ligands have been reported in literature. Among these examples, the family of group 4 complexes bearing the bis(phenolate) ligands with soft-donor sulfur atoms has shown some peculiar features. As a matter of fact, the titanium complexes with 1,4-dithiabutanediyl-linked [OSSO]-type ligands are highly active precatalysts not only for the isospecific polymerization of styrene[10] but also have shown a unique behavior in the homo- and copolymerization of diene monomers.[11] Kol et al., following these results, introduced a methylene group between the S donor and the arene ring, obtaining an improvement of the activity in 1-hexene polymerization with respect to the analogous salan-type complex but with a concomitant loss of stereocontrol.[12] More recently, high isoselectivity in 1-hexene polymerization was achieved by Ishii et al. using a zirconium complex with an [OSSO]-type ligand featuring both methylene and *trans*-1,2-cyclooctanediyl spacers in the molecular backbone.[13] These results clearly show that the activity is profoundly affected by the dimension of the ring. Notably, it resulted that both an increase or a decrease of the number of carbon atom with respect to the cyclooctanediyl ring leads to a decrement of the catalytic activity.[13e]

To further explore these structure−activity relationships in the OSSO ligands with methylene spacers, we turned our attention to OSSO ligands with the phenylene bridge. Moreover, we focused on titanium complexes because this

Received: July 5, 2018
Accepted: September 10, 2018
Published: September 21, 2018

metal is a cost-effective alternative to the other heavier group IV elements. Herein, we report on the synthesis and characterization of new titanium complexes, supported by *o*-phenylene-bridged bis(phenolato) ligands and on their activity as catalyst precursors in ethylene and propylene polymerization.

RESULTS AND DISCUSSION

Synthesis and Crystal Structure. The preligands $OSSO_{tBu}$-H and $OSSO_{Cum}$-H [$OSSO_{tBu}$-H = 6,6′-((1,2-phenylenebis(sulfanediyl))bis(methylene))-bis(2,4-di-*tert*-butyphenol) and $OSSO_{Cum}$-H = 6,6′-((1,2-phenylenebis-(sulfanediyl))bis(methylene))-bis(2,4-bis(2-phenylpropan-2-yl)phenol)] were synthesized following the published procedure, that is, by reaction between the appropriate 2-(bromomethyl)-phenol and benzene-1,2-dithiol.[14] These compounds were recently employed by us for the synthesis of a series of alcoholate group IV complexes that mediated the immortal ROP of L-lactide affording polymers with controlled molecular weights and narrow polydispersity indexes.[14]

Complexes **1**–**2** (**1** = $OSSO_{tBu}TiCl_2$, **2** = $OSSO_{Cum}TiCl_2$) were prepared by the direct reactions of the preligand $OSSO_{tBu}$-H or $OSSO_{Cum}$-H with an equimolar amount of $TiCl_4$ in toluene solution at room temperature, as reported in Scheme 1. Removal of the volatile materials under reduced

Scheme 1. Synthesis of the Phenylene-Bridged $OSSO_R$-H Ligands and of the Corresponding Titanium Complexes 1 and 2

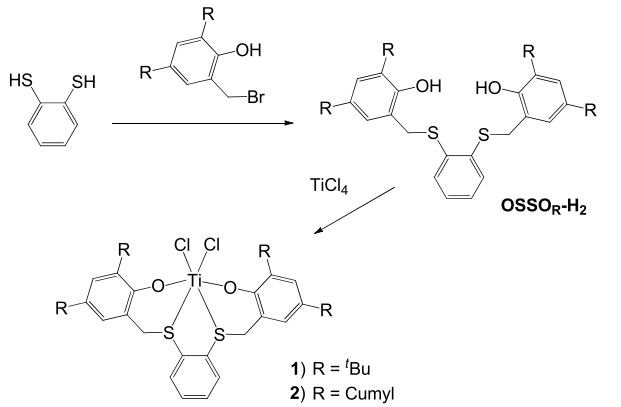

pressure gave red solids, which were recrystallized by acetonitrile affording analytically pure **1**–**2** in high yield (82 and 89%, respectively). Single crystals suitable for X-ray diffraction studies were obtained for complex **1**. The crystal structure of **1** (Figure 1) revealed that the complex possesses an idealized C_2 symmetry with the Ti atom adopting a slightly distorted octahedral coordination.

The [OSSO]-type ligand has the usual *fac*–*fac* wrapping coordination mode, in which the two oxygen atoms are in trans position, the two sulfur atoms are in cis position, and the two chlorides are also mutually cis. The rigidity of the OSSO skeleton causes a distortion of the classical octahedral coordination, forcing the deviation of the O–Ti–O angle from linearity [O1–Ti–O2 161.09(14)°] as it has been found also in the analogous [{L1}Ti(O–^{i}Pr)$_2$] [O–Ti–O 159.76(8)°].[15] The Ti–S distances [Ti–S1 2.601(2); Ti–S2 2.603(2) Å] are shorter than those found in a similar di-isopropoxy Ti(IV) complex bearing an OSSO-type ligand

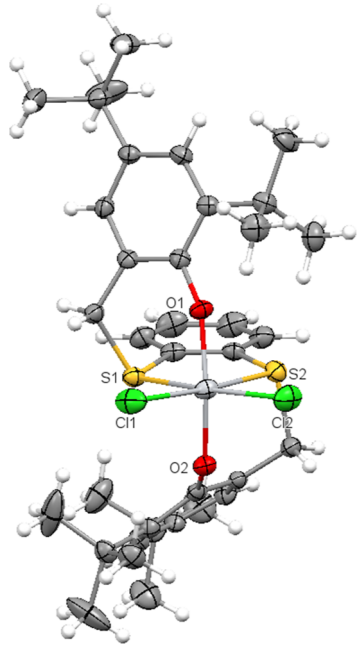

Figure 1. Oak Ridge thermal ellipsoid plot drawing of complex **1** (30% thermal ellipsoids). Selected bond lengths [Å] and bond angles [deg]: Ti–Cl1 = 2.271(2); Ti–Cl2 = 2.278(2); Ti–O1 = 1.835(3); Ti–O2 = 1.864(3); Ti–S1 = 2.601(2); Ti–S2 = 2.603(2); S1–Ti–S2 = 77.88(5); O1–Ti–O2 = 161.09(14); and Cl1–Ti–Cl2 = 104.89(6).

[2.7022(11) and 2.6958(12) Å] but longer than the Ti–S bond lengths [2.5618(9) and 2.5730(8) Å] observed in the dimeric Ti(III) complex bearing two bridging chlorides in addition to the OSSO ligands.[13c] The S1–Ti–S2 bite angle of 77.88(5)° falls in the normal range observed for this kind of angles. The two chlorides are far from each other with an angle of 104.89(6)°.

Solution Structures. The coordination of a tetradentate ligand to a metal center can produce three octahedral stereoisomers, designated as *mer*–*mer* (trans), *fac*–*fac* (cis-α), and *fac*–*mer* (cis-β) belonging to the C_{2v}, C_2, and C_1 point groups, respectively. Cause of the weak bond between the hard titanium center and the soft sulfur atom, [OSSO]–Ti complexes have a stereochemically nonrigid coordination geometry. When dissolved in solution, they may display fluxional processes and/or equilibria between the different stereoisomers. The number of species in solution, their geometry, and the exchange processes of **1** and **2** were investigated with the aid of NMR spectroscopy.

In the ^{1}H NMR spectrum of **1** (1,2-dideutero-1,1,2,2-tetrachloroethane, TCDE, as the solvent), a unique set of the resonances was observed in which the methylene protons of the coordinated ligand resonates as an AB pattern at 4.35 and 3.61 ppm, as expected for diastereotopic protons in a C_2-symmetric environment (Figure S4, Supporting Information). This indicates that, in solution, complex **1** retains the same *fac*–*fac* ligand wrapping to the metal center observed in the solid state. The heating of the solution up to 50 °C produced only a line broadening of the signals. Differently, when the solution of **1** was cooled at subambient temperature, a second pattern of resonances was observed. The methylene protons of this new isomer gave rise to four doublets at δ 4.93, 4.46, 4.32, and 4.00 ppm, suggesting a C_1 symmetry for the metal complex. The ratio between the C_1 and C_2 isomers is 1:4 at

DOI: 10.1021/acsomega.8b01550
ACS Omega 2018, 3, 11608–11616

−40 °C. The exchange process was investigated by appropriate exchange spectroscopy experiments (^{1}H−^{1}H EXSY) at −40 °C (Figure S5, Supporting Information). EXSY peaks between the signals of the methylene groups in each isomer were easily observed. In addition, a second series of less intense cross-peaks correlating the signals of the methylene groups of the two isomers were also detected. These peaks testify a rapid Δ−Λ enantiomer exchange for both the C_1 and C_2 isomers and a slower interconversions between the two geometric C_1 and C_2 isomers.

For the more steric encumbered complex **2**, two sets of signals attesting the presence of the C_1 and C_2 isomers were observed at room temperature (Figure S7, Supporting Information). It is worth noting that the ratio between the C_1 and C_2 isomers is 2:1 at 30 °C. The ^{1}H−^{1}H EXSY (at 30 °C) proved that the Δ−Λ enantiomer exchange and the C_1 and C_2 interconversions occur also in this case (Figure 2).

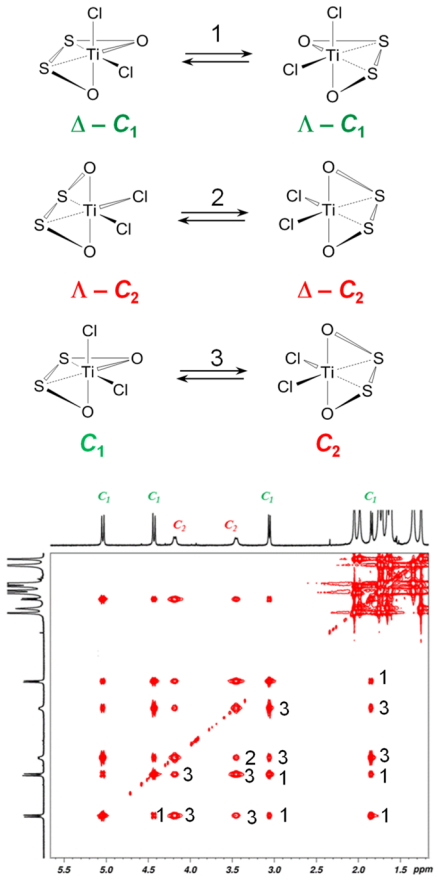

Figure 2. Portion of the ^{1}H−^{1}H EXSY NMR spectrum of **2** (τ_m = 0.300 s, TCDE, 30 °C, and 600 MHz).

This behavior was previously observed for other titanium complexes bearing OSSO ligands containing methylene spacers, that is, ethylene-bridged and cyclooctanediyl-bridged [OSSO]-type ligands. The C_1 symmetric isomer was the prevailing isomer for the ethylene-bridged complex (C_1/C_2 = 1:4),[16] whereas the C_2 symmetric isomer was prevailing for the cyclooctanediyl-bridged complex (C_1/C_2 = 2:1).[13e] Variable-temperature NMR analysis indicates a reversible conversion of two isomers at 60 °C for the titanium dichloro complex with ethylene-bridged [OSSO]-type ligand. For the titanium complex with cyclooctanediyl-bridged [OSSO]-type ligand, the NMR spectrum of the mixtures of isomers was unchanged up to 100 °C.

Polymerization Studies. Complexes **1**−**2** were tested in ethylene polymerization after activation with modified methylaluminoxane (MMAO) or Al^{i}Bu$_3$/[Ph$_3$C][B(C$_6$F$_5$)$_4$] in toluene at room temperature. The main results are summarized in Table 1.

Upon activation with MMAO, both complexes led to active polymerization catalysts. Complex **1** showed an activity of 10 kg mol^{-1} h^{-1}, whereas using complex **2**, the activity increases to 42 kg mol^{-1} h^{-1} (entries 1 and 2, Table 1). The activity of **2** decreases when the [Al]/[Ti] molar ratio is changed from 1000 to 2000 or 500 (entries 3 and 4, Table 1). The obtained polyethylenes (PEs) were scarcely soluble in common aliphatic solvents. For this reason, the polymer products were extracted in boiling xylene and the soluble fractions were characterized by NMR spectroscopy, differential scanning calorimetry (DSC), and gel permeation chromatography (GPC) analysis. All PE samples were linear and showed a melting point of 135 °C. The molecular weight distributions were broad, with very high dispersity indexes ($Đ$), probably because of a partial activation of the active species or to degradation of the catalyst when treated with alkyl aluminum excess.

Treatment with Al-^{i}Bu$_3$ (Al/Ti molar ratio of 20), followed by reaction with 1 equiv of [Ph$_3$C][B(C$_6$F$_5$)$_4$], afforded ethylene polymerization catalysts with activities higher than those obtained with MMAO. Indeed, in the case of complex **1**, an increment of the activity to 59 kg$_{PE}$ mol$_{cat}^{-1}$ bar^{-1} h^{-1} was recorded (entry 5, Table 1). Using complex **2**, with bulky cumyl substituents on the phenol rings, the effect on the catalytic performance is more pronounced, with a fivefold enhancement of the catalytic activity (compare entries 2 and 6, Table 1). With the activity value of 238 kg$_{PE}$·mol$_{cat}^{-1}$·bar^{-1}·h^{-1}, complex **2** can be rated as a highly active catalyst, according to the scale proposed by Gibson.[1b] The comparison between complexes **1** and **2** suggests that increasing the steric hindrance around the metal center leads to a more effective catalytic active species. The DSC analysis of the PEs suggested the formation of highly linear polymers with a melting point of about 122 °C for **2** and of about 130 °C for **1**. The NMR analysis confirmed the linear nature of the obtained polymers. The ^{1}H NMR spectrum of PE by **2** shows a singlet because of the polymethylene sequence at δ 1.16 ppm; a unique signal at δ 28 ppm in the ^{13}C NMR spectrum was parallely observed, and no end group was detected (Figure S11, Supporting Information). The molecular weight distributions of PEs are bimodal and the $Đ$ values are large, probably as a result of different active species (Figure S12, Supporting Information).

Complex **2** was also investigated in propylene polyinsertion. It resulted moderately active at room temperature with an activity value of 3 kg$_{PP}$·mol$_{cat}^{-1}$·bar^{-1}·h^{-1} at 25 °C (entry 7, Table 1) but became inactive at low temperature. The crude products appeared as low melting waxes. In the ^{1}H NMR spectrum signals belonging to unsaturated chain ends were clearly detected (Figure S13, Supporting Information). Two broad resonances at 4.57 and 4.65 ppm and a resonance at 1.60 ppm indicate the presence of vinylidene end group because of β-hydride transfer from the last 1,2 inserted propylene unit. In addition, three complex multiplets at 5.0, 5.4, and 5.8 ppm are due to allylic and *cis*-2-butenyl end groups.[17] Allylic chain end group arises from the β-methyl transfer to the metal center from the last propylene unit inserted with a 1,2-regiochemistry or from the β-hydride transfer from the methyl of the

DOI: 10.1021/acsomega.8b01550
ACS Omega 2018, 3, 11608−11616

Table 1. Ethylene and Propylene Polymerization Results

entry[a]	cocatalyst	Al/Ti	monomer	yield (g)	activity[d]	M_w[e]	$Đ$[e]
1	**1**/MMAO	1000	ethylene	0.49	10	450	76
2	**2**/MMAO	1000	ethylene	2.20	42	1370	56
3	**2**/MMAO	2000	ethylene	0.26	5	940	76
4	**2**/MMAO	500	ethylene	0.17	3	1340	51
5[b]	**1**/Al^{i}Bu$_3$/[Ph_3C][$B(C_6F_5)_4$]	20	ethylene	1.48	59	1190	71
6[b]	**2**/Al^{i}Bu$_3$/[Ph_3C][$B(C_6F_5)_4$]	20	ethylene	5.94	238	110	32
7[c]	**2**/Al^{i}Bu$_3$/[Ph_3C][$B(C_6F_5)_4$]	20	propylene	0.15	3		

[a]Polymerization conditions: complex = 10 μmol ([Ti] = 1.0×10^{-4} M), cocatalyst = 10 mmol of MMAO, 100 mL of toluene, monomer pressure = 5 atm, temperature = 25 °C, and polymerization time = 1 h. [b]Polymerization conditions: complex = 10 μmol ([Ti] = 1.0×10^{-4} M), cocatalyst = 10 μmol of [Ph_3C][$B(C_6F_5)_4$] (B/Ti = 1) and 0.2 mmol of Al^{i}Bu$_3$, 100 mL of toluene, monomer pressure = 5 atm, temperature = 25 °C, and polymerization time = 0.5 h. [c]Polymerization time = 1 h. [d]$kg_{PE}\ mol_{cat}^{-1}\ bar^{-1}\ h^{-1}$. [e]Determined by GPC with respect to polystyrene standard.

propylene unit inserted with a 2,1-regiochemistry. *cis*-2-Butenyl end group is due to the β-hydride transfer from the last inserted propylene unit with 2,1 regiochemistry after 1,2 insertion. A minor signal because of the 3-butenyl chain end group is also detected; this group comes from the β-hydride transfer from the methyl of the last inserted propylene unit with 2,1 regiochemistry after 1,2 insertion.

The signals diagnostic of these terminations were also detected in the ^{13}C NMR spectrum of the oligomers obtained by **2** (Figure 3). Vinylidene (44%) and allyl (39%) end groups are the principal end groups, and *cis*-2-butenyl and 3-butenyl end groups amount to 14 and 3%, respectively.

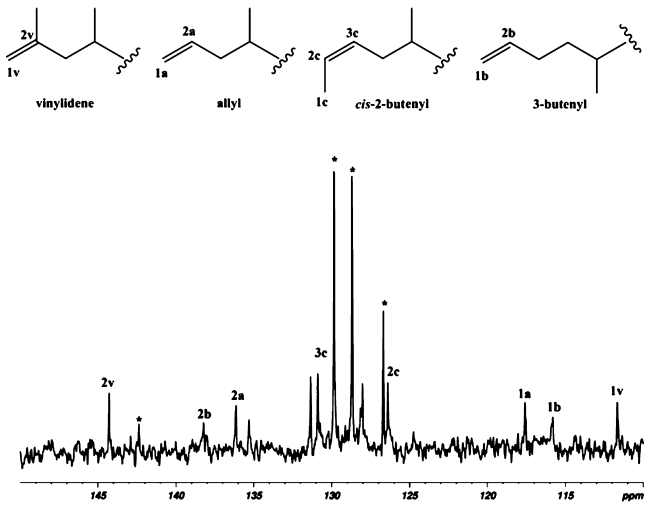

Figure 3. ^{13}C NMR spectrum of olefinic region of polypropylene oligomers sample from run 7 in Table 1 ($CDCl_3$, 25 °C, and 75 MHz). Signals marked with * are due to Ph_3CH.

The ^{13}C NMR analysis of oligopropylene showed an atactic microstructure, as revealed by the pattern of signals in the methyl pentad region. The regioregularity of the monomer insertion was not elevated. The signals in the ranges of 34.1−35.6 and 14.7−17.2 ppm because of the methylene carbons of the tail-to-tail sequence and methyl carbons of the head-to-head concatenation were observed with approximately the same area giving a total amount of regioirregular sequences of 27%.

Molecular Modeling Studies. To shed light on the polymerization mechanism promoted by the title catalytic systems, a density functional theory (DFT) study was carried out. We investigated chain propagation and chain termination, the elementary steps involved in the reaction, using as a model of the active species the cationic *n*-propyl complex deriving from the C_2 isomer of **1** ($\mathbf{A}_{C_2}$). The energy profile is displayed in Figure 4.

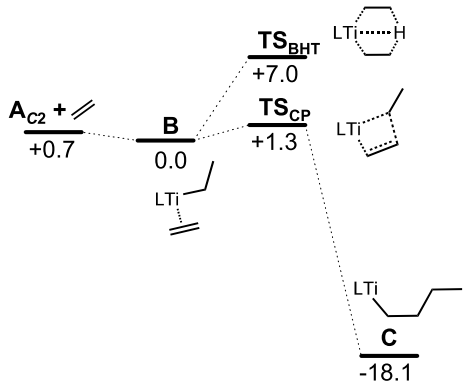

Figure 4. Calculated pathways for ethylene insertion and β-hydrogen transfer to the monomer (BHT). Energies are given in kcal mol^{-1}.

According to the coordination insertion mechanism, the ethylene coordination to the active species leads to the π-complex **B**, from which both chain propagation and chain termination can start. The coordination energy of ethylene is quite low (−0.7 kcal/mol). The propagation reaction proceeds through the insertion of ethylene into the metal−carbon bond. This step requires overcoming a quite low barrier of 1.3 kcal/mol (Figure 4) and involves the four-membered transition state $\mathbf{TS}_{CP}$ (Figure 5).

The resulting insertion product **C** is more stable than **B** by −18.1 kcal/mol. Alternately, the π-complex **B** can lead to the termination of the growing polymer chain through the β-hydrogen transfer to the monomer (BHT). The process involves the migration of a hydrogen atom in the β position belonging to the alkyl chain to the nearest carbon atom of the monomer. The corresponding transition state $\mathbf{TS}_{BHT}$ reminds a bis(olefin) complex, characterized by a strong metal−hydrogen interaction. As a matter of fact, the distance between the metal atom and the hydrogen atom moving from the alkyl group to the monomer was found to be 1.91 Å (Figure 5). The barrier associated with this step is 7.0 kcal/mol. A second termination process is the β-hydrogen elimination (BHE). Lacking the coordinated monomer, one of the hydrogen atom of the alkyl chain in β-position can move to the metal center. It is generally reported that BHE is not the preferential chain termination reaction in the ethylene polymerization promoted by OSSO-

DOI: 10.1021/acsomega.8b01550
ACS Omega 2018, 3, 11608−11616

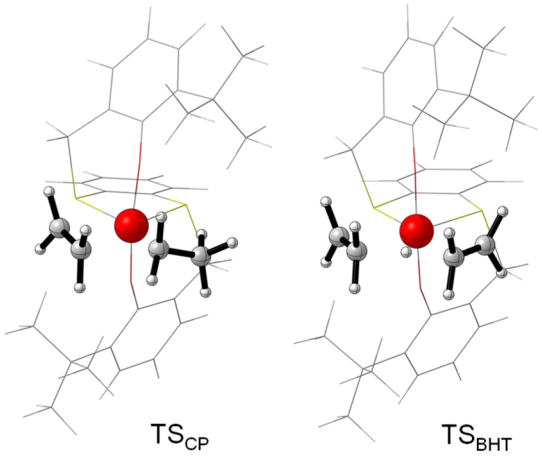

Figure 5. Geometries of the transition-state $\mathbf{TS}_{CP}$ and $\mathbf{TS}_{BHT}$.

type complex reactions because of its substantially higher activation energy compared to the BHT process.[18] For this reason, the barrier for this step was not calculated. The balance between β-hydrogen transfer and chain propagation has a direct consequence on the catalytic behavior: more competitive the BHT process is, longer polymeric chains are. An estimation of the competition between the two process is given by the different heights of the corresponding activation barriers ($\Delta\Delta E^{\#}_{BHT\text{-}CP}$). The $\Delta\Delta E^{\#}_{BHT\text{-}CP}$ for title catalytic system is 5.7; this value indicates that our catalyst system is prone in producing long polymeric chains in agreement with the experimental results.

It should be noted that the prototypal titanium complex dichloro{1,4-dithiabutanediyl-2,2′-bis(4,6-di-*tert*-butylphenoxy)}titanium (**3**), activated with MAO, leads to high-molecular-weight-branched PE.[19] Experimental evidence supported by DFT calculations suggested that the mechanism involves the in situ formation of α-olefins by β-hydride elimination followed by the reinsertion of these α-olefins during the propagation step.[18,19] The insertion and the BHT barriers computed for **3** at the same level of theory were lower than those obtained for our model complex: the insertion barrier was 1.0 kcal/mol, whereas the BHE barrier was 5.9 kcal/mol and the corresponding $\Delta\Delta E^{\#}_{BHT\text{-}CP}$ for **3** is 4.9 kcal/mol.[18] Thus, different polymeric architecture obtained by these catalysts can be addressed to the more competitive termination process found for complex **3** with respect to the catalytic system reported in this study.

The multimodal GPC traces of polymers obtained with our catalytic systems suggest the formation of multiple catalytically active species having different polymerization performances. Even though the origin of multimodality is still not completely clear and it is necessary to use caution in deducing the real active species from the solution structures of the precatalysts, we wonder if the coordination isomerism of the precatalysts could cause the broadening of the molecular weight distribution. Thus, we turn our attention to the other possible geometric isomers of the active species, that is, the isomer with a *mer*−*mer* wrapping of the OSSO ligand around the metal center ($\mathbf{A}_{C_{2v}}$) and the isomer with an *fac*−*mer* wrapping of the OSSO ligand ($\mathbf{A}_{C_1}$). $\mathbf{A}_{C_{2v}}$ would not lead to insertion because it could only capture an olefin trans to the alkyl group; therefore, it was not further considered. $\mathbf{A}_{C_{2v}}$ was successfully optimized and showed very similar energy respect to $\mathbf{A}_{C_2}$, but all our attempts to locate the corresponding ethylene coordination adduct were unsuccessful. The potential energy curve resulting from the nearing of ethylene to the titanium atom of $\mathbf{A}_{C_2}$ presented a minimum when the ethylene was placed at about 5.0 Å from the titanium atom, a distance coherent with the formation of a van der Waals adduct, not with a coordination adduct. Thus, $\mathbf{A}_{C_{2v}}$ and $\mathbf{A}_{C_1}$ should only represent inactive/dormant species that do not influence the distribution of the molecular weights. In light of these observations, the formation of multiple active species would derive from partial transformation of the precatalyst structure by the aluminum cocatalyst.

CONCLUSIONS

The dichloro titanium complexes **1**−**2**, supported by [OSSO]-type ligands with an *o*-phenylene-bridge, were prepared and completely characterized in solution by NMR spectroscopy. For complex **1**, the X-ray crystal structure revealed that the titanium complex has a C_2-symmetric conformation with a distorted octahedral geometry about the titanium center. In solution, **1** mainly maintained the C_2 symmetric structure while **2** displayed an equilibrium between C_2- and C_1-symmetric stereoisomers.

Upon activation with MMAO, these complexes were found to be active for ethylene polymerization. The use of $[Ph_3C][B(C_6F_5)_4]$, in the presence of Al^iBu_3 as an alkylating agent and a scavenger, produced much more active catalysts; in particular, complex **2** showed a high activity of 238 $kg_{PE}\cdot mol_{cat}^{-1}\cdot bar^{-1}\cdot h^{-1}$. Linear high-molecular-weight PEs were obtained with broad dispersity indexes, probably because of the presence of different active species in solution.

DFT investigation on the elementary steps of the polymerization process revealed that the β-hydrogen transfer to the monomer, the principal termination process, is not competitive with respect to propagation, explaining the production of long polymer chains. The $\Delta\Delta E^{\#}_{BHT\text{-}CP}$ values for our catalytic system are higher than that computed for the prototypal titanium complex **3**, in agreement with the different polymeric architecture obtained by these catalysts. Moreover, we found that the multimodal molecular weight distribution cannot be addressed to the coordination isomerism of the precatalysts as only the active species deriving from the C_2 isomer is catalytically active, whereas the other possible species are inactive/dormant species.

The precatalyst **2** was also active in propene polymerization at room temperature, producing atactic oligomers terminated with unsaturated end groups.

EXPERIMENTAL SECTION

Materials and Methods. The description of the general procedures, the standard techniques, and instruments employed is provided in the Supporting Information. The compounds 6,6′-((1,2-phenylenebis(sulfanediyl))bis(methylene))bis(2,4-di-*tert*-butyphenol) ($OSSO_{tBu}$-H) and 6,6′-((1,2-phenylenebis(sulfanediyl))bis(methylene))bis(2,4-bis(2-phenylpropan-2-yl)phenol) ($OSSO_{Cum}$-H) were synthesized following the literature procedure.[14]

Synthesis of the Complex ($OSSO_{tBu}$)$TiCl_2$ (1). A solution of $TiCl_4$ (0.86 mmol, 90 μL) in toluene (4 mL) was added dropwise to a toluene solution (6 mL) of $OSSO_{tBu}$-H (0.50 g; 0.86 mmol) at 25 °C. The mixture was left under stirring for 2 h, and the solvent was distilled off in vacuum. The

DOI: 10.1021/acsomega.8b01550
ACS Omega 2018, 3, 11608−11616

red residue was crystallized from acetonitrile at 25 °C (0.41 g, 82%). Spectroscopic data: ^{1}H NMR (C_6D_6, 25 °C, 300 MHz): δ 7.34 (br s, 2H, Ar), 6.60 (br s, 2H, Ar), 6.49 (br s, 2H, Ar), 6.09 (m, 2H, Ar), 4.39 (d, J_{HH} = 13.4 Hz, 2H, C*H*−H), 3.48 (br sd, 2H, C*H*−H), 1.89 (s, 18H, CH_3), 1.03 (s, 18H, CH_3). ^{1}H NMR (TCDE, 25 °C, 600 MHz): δ 7.37 (br s, 2H, Ar), 7.29 (br s, 2H, Ar), 7.14 (br s, 2H, Ar), 6.25 (br s, 2H, Ar), 4.50 (d, J_{HH} = 13.1 Hz, 2H, C*H*−H), 3.73 (d, J_{HH} = 13.1 Hz, 2H, C*H*−H), 1.59 (s, 18H, CH_3), 1.06 (s, 18H, CH_3). ^{13}C NMR (CD_2Cl_2, 25 °C, 75.5 MHz): δ 162.1, 144.6, 137.5, 136.3, 135.2, 131.8, 126.2, 124.7, 122.9, 43.2, 35.8, 34.7, 31.5, 30.9. Anal. Calcd for $C_{36}H_{48}Cl_2O_2S_2Ti$: C, 62.15; H, 6.95; S, 9.22. Found: C, 62.07; H, 6.99; S, 9.14.

Synthesis of the Complex ($OSSO_{Cum}$)$TiCl_2$ (2). A solution of $TiCl_4$ (1.11 mmol, 120 μL) in toluene (8 mL) was added dropwise to a toluene solution (12 mL) of $OSSO_{Cum}$-H (0.92 g; 1.11 mmol) at 25 °C. The mixture was stirred for 2 h, and the solvent was distilled off in vacuum. The red residue was crystallized from acetonitrile at 25 °C (0.81 g, 89%). Spectroscopic data: ^{1}H NMR (TCDE, 25 °C, 600 MHz): δ 7.45 (s, Ar), 7.42−7.05 (m, Ar), 6.97 (m, Ar), 6.85−6.70 (m, Ar), 6.68 (s, Ar), 6.60 (t, Ar), 6.21 (d, Ar), 6.14 (br s, Ar), 5.07 (d, J_{HH} = 15.1 Hz, C*H*−H_{C1}), 4.45 (d, J_{HH} = 15.1 Hz, C*H*−H_{C1}), 4.22 (d, J_{HH} = 12.0 Hz, C*H*−H_{C2}), 3.48 (d, J_{HH} = 12.0 Hz, C*H*−H_{C2}), 3.08 (d, J_{HH} = 11.3 Hz, C*H*−H_{C1}), 2.08 (s, CH_3), 2.01 (s, CH_3), 1.87 (d, J_{HH} = 12.0 Hz, C*H*−H_{C1}), 1.78 (s, CH_3), 1.74 (s, CH_3), 1.68 (s, CH_3), 1.65 (s, CH_3), 1.63 (s, CH_3), 1.37 (s, CH_3), 1.28 (s, CH_3), 1.12 (s, CH_3). ^{13}C NMR (CD_2Cl_2, 25 °C, 75.5 MHz): δ 162.9, 161.7, 160.1, 152.0, 151.3, 150.9, 150.5, 145.2, 129.2, 128.7, 128.5, 128.3, 128.1, 127.6, 127.4, 127.2, 127.0, 126.8, 125.7, 43.3, 43.1, 43.0, 41.8, 39.8, 36.4, 33.2, 31.7, 31.2, 31.0, 30.6, 29.1, 28.2, 27.1. Anal. Calcd for $C_{56}H_{56}Cl_2O_2S_2Ti$: C, 71.25; H, 5.98; S, 6.79. Found: C, 71.29; H, 6.02; S, 6.72.

Procedure for Ethylene Polymerization Using MMAO. Ethylene polymerizations were carried out in a 250 mL Buchi glass reactor equipped with a mechanical stirrer. In a typical procedure, the reactor vessel was charged with a toluene solution of MMAO (0.1 M, 90 mL), pressurized with ethylene and vented three times. After the mixture was thermostated at the required temperature and 1 atm of ethylene, a toluene solution of precatalyst (10 μmol in 10 mL) was injected into the reactor, and the ethylene was rapidly charged to the prescribed pressure. After the specific reaction time, ethylene was evacuated and the polymerization mixture was poured in ethanol acidified with aqueous HCl. The solid polymer was collected by filtration, washed with fresh ethanol, and dried in a vacuum drying oven at 80 °C.

Procedure for Ethylene and Propylene Polymerization Using (Ph_3C)[$B(C_6F_5)_4$]. Ethylene polymerizations were carried out in a 250 mL Buchi glass reactor equipped with a mechanical stirrer. In a typical procedure, the reactor vessel was charged with a toluene solution of Al^iBu_3 (0.2 mmol in 90 mL), pressurized with the gaseous monomer and vented three times. After the mixture was thermostated at the required temperature and 1 atm of monomer, a toluene solution (10 mL) of precatalyst (10 μmol) and (Ph_3C)[$B(C_6F_5)_4$] (5.6 mg, 10 μmol) was injected into the reactor, and the monomer was rapidly charged to the prescribed pressure. After the specific reaction time, the gaseous monomer was evacuated and the polymerization mixture was poured in ethanol acidified with aqueous HCl. The solid polymer was collected by filtration, washed with fresh ethanol, and dried in a vacuum drying oven at 80 °C.

In the case of propylene polymerization promoted by **2**, oligomers were extracted from the oligomerization reaction with $CHCl_3$ and dried on $MgSO_4$. The excess solvent was distilled off at reduced pressures.

Computational Details. DFT calculations were performed with the Gaussian 09 program suite.[20] All geometrical optimizations were performed at the BP86 level, that is, employing the exchange−correlation functionals of Becke and Perdew,[21] respectively. The electronic configuration was described with the quasi-relativistic LANL2DZ[22] effective core potential for Ti and S, whereas we adopted the SVP[23] basis set for O, C, and H. To save computational resources, the alkyl groups of the OSSO ligand in ortho position were modeled with the *tert*-butyl groups, whereas the alkyl groups in para position were replaced by hydrogen atoms. The structures of transition states were located by applying Schlegel's synchronous transit-guided quasi-Newton (QST2) method as implemented in Gaussian 09. All geometries were characterized as minimum or transition state through frequency calculations. The differences in energy reported in Figure 4 are in the gas phase without zero-point correction. Cartesian coordinates of all DFT optimized structures are available on request. Structures were visualized by the CYLview program.[24]

Single-Crystal X-ray Crystallography. The details of the data collection for ($OSSO_{tBu}$)$TiCl_2$ (**1**) are given in the Supporting Information. Crystal data are reported in Table 2.

Table 2. Crystal Data and Structure Refinement for ($OSSO_{tBu}$)$TiCl_2$

empirical formula	$C_{36}H_{48}Cl_2O_2S_2Ti$
formula weight	695.66
temperature/K	296(2)
crystal system	monoclinic
space group	$P2_1/c$
a, Å	14.2494(6)
b, Å	15.1062(7)
c, Å	17.1323(7)
α, deg	90
β, deg	101.223(3)
γ, deg	90
cell volume, Å^3	3617.3(3)
Z	4
ρ_c, mg m^{-3}	1.277
μ(Mo Kα), mm^{-1}	0.530
F(000)	1472
crystal size mm	0.15 × 0.10 × 0.10
θ limits, deg	1.457 to 24.498
Refl. collected, unique (R_{int})	50 482/6012 (0.2416)
goodness-of-fit on F^2	1.109
$R_1(F)$[a], $wR_2(F^2)$ [$I > 2\sigma(I)$][b]	0.0581, 0.0830
largest diff. peak and hole, e·Å^{-3}	0.316 and −0.400

[a] $R_1 = \Sigma||F_o| - |F_c||/\Sigma|F_o|$. [b] $wR_2 = [\Sigma w(F_o^2 - F_c^2)^2/\Sigma w(F_o^2)^2]^{1/2}$ where $w = 1/[\sigma 2(F_o^2) + (aP)^2 + bP]$ where $P = (F_o^2 + F_c^2)/3$.

CCDC 1578280 contains the supplementary crystallographic data for this paper. These data can be obtained free of charge from the Cambridge Crystallographic Data Centre via www.ccdc.cam.ac.uk/data_request/cif.

DOI: 10.1021/acsomega.8b01550
ACS Omega 2018, 3, 11608−11616

■ ASSOCIATED CONTENT

Supporting Information

The Supporting Information is available free of charge on the ACS Publications website at DOI: 10.1021/acsomega.8b01550.

Description of the general procedures; figures giving ^{1}H NMR spectra of proligands, complexes, and polymers; GPC trace of PE sample; and crystallographic details for complex **1** (PDF)

Crystallographic data for $(OSSO_{tBu})TiCl_2$ (CIF)

■ AUTHOR INFORMATION

Corresponding Author

*E-mail: smilione@unisa.it (S.M.).

ORCID

Antonio Buonerba: 0000-0003-1101-3248

Francesco Della Monica: 0000-0001-6530-7351

Alfonso Grassi: 0000-0002-2664-3114

Carmine Capacchione: 0000-0001-7254-8620

Stefano Milione: 0000-0002-3473-1480

Notes

The authors declare no competing financial interest.

■ ACKNOWLEDGMENTS

Ministero dell'Istruzione dell'Università e della Ricerca is acknowledged for the financial support (MIUR, Roma, Italy for FARB 2016). M.M. thanks the University of Bologna for the financial support. The authors are also grateful to Dr. Patrizia Oliva and Dr. Patrizia Iannece from the University of Salerno for technical assistance. HTExplore, a spin-off of the Federico II University of Naples (Italy), is also acknowledged for the high-temperature GPC measurements.

■ REFERENCES

(1) (a) Gibson, V. C.; Spitzmesser, S. K. Advances in Non-Metallocene Olefin Polymerization Catalysis. *Chem. Rev.* **2003**, *103*, 283−316. (b) Britovsek, G. J. P.; Gibson, V. C.; Wass, D. F. The Search for New-Generation Olefin Polymerization Catalysts: Life beyond Metallocenes. *Angew. Chem., Int. Ed.* **1999**, *38*, 428−447. (c) Matsugi, T.; Fujita, T. High-performance olefin polymerization catalysts discovered on the basis of a new catalyst design concept. *Chem. Soc. Rev.* **2008**, *37*, 1264−1277. (d) Domski, G. J.; Rose, J. M.; Coates, G. W.; Bolig, A. D.; Brookhart, M. Living Alkene Polymerization: New Methods for the Precision Synthesis of Polyolefins. *Prog. Polym. Sci.* **2007**, *32*, 30−92. (e) Carpentier, J.-F. When Single-Site Polymerization Catalysis Meets Chirality: Optical Activity of Stereoregular Polyolefins. *Angew. Chem., Int. Ed.* **2007**, *46*, 6404−6406. (f) Busico, V. Metal-catalysed olefin polymerisation into the new millennium: a perspective outlook. *Dalton Trans.* **2009**, *0*, 8794−8802. (g) Corradini, P.; Guerra, G.; Cavallo, L. Do New Century Catalysts Unravel the Mechanism of Stereocontrol of Old Ziegler−Natta Catalysts? *Acc. Chem. Res.* **2004**, *37*, 231−241. (h) Coates, G. W.; Hustad, P. D.; Reinartz, S. Catalysts for the Living Insertion Polymerization of Alkenes: Access to New Polyolefin Architectures Using Ziegler-Natta Chemistry. *Angew. Chem., Int. Ed.* **2002**, *41*, 2236−2257. (i) Coates, G. W. Precise Control of Polyolefin Stereochemistry Using Single-Site Metal Catalysts. *Chem. Rev.* **2000**, *100*, 1223−1252.

(2) (a) Makio, H.; Fujita, T. *Stereoselective Polymerization with Single-Site Catalysts*; CRC Press, Boca Raton, FL, 2008; pp 157−168. (b) Baier, M. C.; Zuideveld, M. A.; Mecking, S. Post-Metallocenes in the Industrial Production of Polyolefins. *Angew. Chem., Int. Ed.* **2014**, *53*, 9722−9744.

(3) (a) Matsui, S.; Mitani, M.; Saito, J.; Tohi, Y.; Makio, H.; Matsukawa, N.; Takagi, Y.; Tsuru, K.; Nitabaru, M.; Nakano, T.; Tanaka, H.; Kashiwa, N.; Fujita, T. A Family of Zirconium Complexes Having Two Phenoxy−Imine Chelate Ligands for Olefin Polymerization. *J. Am. Chem. Soc.* **2001**, *123*, 6847−6856. (b) Makio, H.; Terao, H.; Iwashita, A.; Fujita, T. FI Catalysts for Olefin Polymerization-A Comprehensive Treatment. *Chem. Rev.* **2011**, *111*, 2363−2449.

(4) (a) Tian, J.; Coates, G. W. Development of a Diversity-Based Approach for the Discovery of Stereoselective Polymerization Catalysts: Identification of a Catalyst for the Synthesis of Syndiotactic Polypropylene. *Angew. Chem., Int. Ed.* **2000**, *39*, 3626−3629. (b) Tian, J.; Hustad, P. D.; Coates, G. W. A New Catalyst for Highly Syndiospecific Living Olefin Polymerization: Homopolymers and Block Copolymers from Ethylene and Propylene. *J. Am. Chem. Soc.* **2001**, *123*, 5134−5135. (c) Hustad, P. D.; Tian, J.; Coates, G. W. Mechanism of Propylene Insertion Using Bis(phenoxyimine)-Based Titanium Catalysts: An Unusual Secondary Insertion of Propylene in a Group IV Catalyst System. *J. Am. Chem. Soc.* **2002**, *124*, 3614−3621.

(5) (a) Tshuva, E. Y.; Goldberg, I.; Kol, M. Isospecific Living Polymerization of 1-Hexene by a Readily Available Nonmetallocene C2-Symmetrical Zirconium Catalyst. *J. Am. Chem. Soc.* **2000**, *122*, 10706−10707. (b) Segal, S.; Goldberg, I.; Kol, M. Zirconium and Titanium Diamine Bis(phenolate) Catalysts for α-Olefin Polymerization: From Atactic Oligo(1-hexene) to Ultrahigh-Molecular-Weight Isotactic Poly(1-hexene). *Organometallics* **2005**, *24*, 200−202. (c) Cohen, A.; Kopilov, J.; Goldberg, I.; Kol, M. C1-Symmetric Zirconium Complexes of [ONNO′]-Type Salan Ligands: Accurate Control of Catalyst Activity, Isospecificity, and Molecular Weight in 1-Hexene Polymerization. *Organometallics* **2009**, *28*, 1391−1405.

(6) (a) Meppelder, G.-J. M.; Fan, H.-T.; Spaniol, T. P.; Okuda, J. Group 4 Metal Complexes Supported by [ONNO]-Type Bis(o-aminophenolato) Ligands: Synthesis, Structure, and α-Olefin Polymerization Activity. *Organometallics* **2009**, *28*, 5159−5165. (b) Sergeeva, E.; Kopilov, J.; Goldberg, I.; Kol, M. Salan Ligands Assembled Around Chiral Bipyrrolidine: Predetermination of Chirality Around Octahedral Ti and Zr Centres. *Chem. Commun.* **2009**, *0*, 3053−3055. (c) Cohen, A.; Yeori, A.; Kopilov, J.; Goldberg, I.; Kol, M. Construction of C1-symmetric zirconium complexes by the design of new Salan ligands. Coordination chemistry and preliminary polymerisation catalysis studies. *Chem. Commun.* **2008**, *0*, 2149−2151. (d) Segal, S.; Yeori, A.; Shuster, M.; Rosenberg, Y.; Kol, M. Isospecific Polymerization of Vinylcyclohexane by Zirconium Complexes of Salan Ligands. *Macromolecules* **2008**, *41*, 1612−1617. (e) Gendler, S.; Zelikoff, A. L.; Kopilov, J.; Goldberg, I.; Kol, M. Titanium and Zirconium Complexes of Robust Salophan Ligands. Coordination Chemistry and Olefin Polymerization Catalysis. *J. Am. Chem. Soc.* **2008**, *130*, 2144−2145. (f) Yeori, A.; Goldberg, I.; Shuster, M.; Kol, M. Diastereomerically-Specific Zirconium Complexes of Chiral Salan Ligands: Isospecific Polymerization of 1-Hexene and 4-Methyl-1-pentene and Cyclopolymerization of 1,5-Hexadiene. *J. Am. Chem. Soc.* **2006**, *128*, 13062−13063. (g) Busico, V.; Cipullo, R.; Pellecchia, R.; Ronca, S.; Roviello, G.; Talarico, G. Design of stereoselective Ziegler-Natta propene polymerization catalysts. *Proc. Natl. Acad. Sci. U.S.A.* **2006**, *103*, 15321−15326. (h) Strianese, M.; Lamberti, M.; Mazzeo, M.; Tedesco, C.; Pellecchia, C. Polymerization of ethylene and propene promoted by binaphthyl-bridged Schiff base complexes of titanium. *J. Mol. Catal. A: Chem.* **2006**, *258*, 284−291. (i) Yeori, A.; Groysman, S.; Goldberg, I.; Kol, M. Diastereoisomerically Selective Enantiomerically Pure Titanium Complexes of Salan Ligands: Synthesis, Structure, and Preliminary Activity Studies. *Inorg. Chem.* **2005**, *44*, 4466−4468. (j) Groysman, S.; Sergeeva, E.; Goldberg, I.; Kol, M. Salophan Complexes of Group IV Metals. *Eur. J. Inorg. Chem.* **2005**, 2480−2485. (k) Lamberti, M.; Consolmagno, M.; Mazzeo, M.; Pellecchia, C. A Binaphthyl-Bridged Salen Zirconium Catalyst Affording Atactic Poly(propylene) and Isotactic Poly(α-olefins). *Macromol. Rapid Commun.* **2005**, *26*, 1866−1871. (l) Yeori, A.; Gendler, S.; Groysman, S.; Goldberg, I.; Kol, M.

Salalen: a hybrid Salan/Salen tetradentate [ONNO]-type ligand and its coordination behavior with group IV metals. *Inorg. Chem. Commun.* **2004**, *7*, 280−282. (m) Balsells, J.; Carroll, P. J.; Walsh, P. J. Achiral Tetrahydrosalen Ligands for the Synthesis ofC2-Symmetric Titanium Complexes: A Structure and Diastereoselectivity Study. *Inorg. Chem.* **2001**, *40*, 5568−5574.

(7) Nakata, N.; Toda, T.; Ishii, A. Recent advances in the chemistry of Group 4 metal complexes incorporating [OSSO]-type bis(phenolato) ligands as post-metallocene catalysts. *Polym. Chem.* **2011**, *2*, 1597−1610.

(8) (a) Frediani, M.; Sémeril, D.; Comucci, A.; Bettucci, L.; Frediani, P.; Rosi, L.; Matt, D.; Toupet, L.; Kaminsky, W. Ultrahigh-Molecular-Weight Polyethylene by Using a Titanium Calix[4]arene Complex with High Thermal Stability under Polymerization Conditions. *Macromol. Chem. Phys.* **2007**, *208*, 938−945. (b) de S. Basso, N. R.; Greco, P. P.; Carone, C. L. P.; Livotto, P. R.; Simplício, L. M. T.; da Rocha, Z. N.; Galland, G. B.; dos Santos, J. H. Z. Reactivity of Zirconium and Titanium Alkoxides Bidentate Complexes on Ethylene Polymerization. *J. Mol. Catal. A: Chem.* **2007**, *267*, 129−136. (c) Suzuki, Y.; Oshiki, T.; Tanaka, H.; Takai, K.; Fujita, T. A Novel Heteroligated Phenoxy-based Titanium Complex: Structure, Stability, and Ethylene Polymerization Behavior. *Chem. Lett.* **2005**, *34*, 1458−1459. (d) Suzuki, Y.; Inoue, Y.; Tanaka, H.; Fujita, T. Phenoxy-Ether Ligated Ti Complexes for the Polymerization of Ethylene. *Macromol. Rapid Commun.* **2004**, *25*, 493−497. (e) Carone, C.; de Lima, V.; Albuquerque, F.; Nunes, P.; de Lemos, C.; dos Santos, J. H. Z.; Galland, G. B.; Stedile, F. C.; Einloft, S.; de S. Basso, N. R. Zirconium Alkoxide Complexes as Catalysts for Ethylene Polymerization. *J. Mol. Catal. A: Chem.* **2004**, *208*, 285−290. (f) Capacchione, C.; Neri, P.; Proto, A. Polymerization of ethylene in the presence of 1,3-dimethoxy-p-But-calix[4]arene titanium dichloride. NMR evidence of the cationic titanium compound generated by methylalumoxane. *Inorg. Chem. Commun.* **2003**, *6*, 339−342.

(9) (a) Long, R. J.; Jones, D. J.; Gibson, V. C.; White, A. J. P. Zirconium Complexes Containing Tetradentate O,P,P,O Ligands: Ethylene and Propylene Polymerization Studies. *Organometallics* **2008**, *27*, 5960−5967. (b) Long, R. J.; Gibson, V. C.; White, A. J. P. Group 4 Metal Olefin Polymerization Catalysts Stabilized by Bidentate O,P Ligands. *Organometallics* **2008**, *27*, 235−245. (c) Long, R. J.; Gibson, V. C.; White, A. J. P.; Williams, D. J. Combining Hard and Soft Donors in Early-Transition-Metal Olefin Polymerization Catalysts. *Inorg. Chem.* **2006**, *45*, 511−513. (d) Hanaoka, H.; Imamoto, Y.; Hino, T.; Oda, Y. Synthesis and characterization of phosphorous-bridged bisphenoxy titanium complexes and their application to ethylene polymerization. *J. Organomet. Chem.* **2006**, *691*, 4968−4974.

(10) (a) Capacchione, C.; Proto, A.; Ebeling, H.; Mülhaupt, R.; Möller, K.; Spaniol, T. P.; Okuda, J. Ancillary Ligand Effect on Single-Site Styrene Polymerization: Isospecificity of Group 4 Metal Bis(phenolate) Catalysts. *J. Am. Chem. Soc.* **2003**, *125*, 4964−4965. (b) Capacchione, C.; Manivannan, R.; Barone, M.; Beckerle, K.; Centore, R.; Oliva, L.; Proto, A.; Tuzi, A.; Spaniol, T. P.; Okuda, J. Isospecific Styrene Polymerization by Chiral Titanium Complexes That Contain a Tetradentate [OSSO]-Type Bis(phenolato) Ligand. *Organometallics* **2005**, *24*, 2971−2982.

(11) (a) Okuda, S.; Cuomo, C.; Capacchione, C.; Zannoni, C.; Grassi, A.; Proto, A. Stereoselective Polymerization of Conjugated Dienes and Styrene−Butadiene Copolymerization Promoted by Octahedral Titanium Catalyst. *Macromolecules* **2007**, *40*, 5638−5643. (b) Capacchione, C.; Avagliano, A.; Proto, A. Ethylene−Butadiene Copolymerization Promoted by Titanium Complex Containing a Tetradentate [OSSO]-Type Bis(phenolato) Ligand. *Macromolecules* **2008**, *41*, 4573−4575. (c) Proto, A.; Avagliano, A.; Saviello, D.; Capacchione, C. Copolymerization of Ethylene with 4-Methyl-1,3-pentadiene Promoted by Titanium Complexes Containing a Tetradentate [OSSO]-Type Bis(phenolato) Ligand. *Macromolecules* **2009**, *42*, 6981−6985. (d) Proto, A.; Avagliano, A.; Saviello, D.; Ricciardi, R.; Capacchione, C. Living, Isoselective Polymerization of Styrene and Formation of Stereoregular Block Copolymers via Sequential Monomer Addition. *Macromolecules* **2010**, *43*, 5919−5921. (e) Capacchione, C.; Saviello, D.; Avagliano, A.; Proto, A. Copolymerization of ethylene with isoprene promoted by titanium complexes containing a tetradentate [OSSO]-type bis(phenolato) ligand. *J. Polym. Sci., Part A: Polym. Chem.* **2010**, *48*, 4200−4206. (f) Capacchione, C.; Saviello, D.; Ricciardi, R.; Proto, A. Living, Isoselective Polymerization of 4-Methyl-1,3-pentadiene and Styrenic Monomers and Synthesis of Highly Stereoregular Block Copolymers via Sequential Monomer Addition. *Macromolecules* **2011**, *44*, 7940−7947. (g) Costabile, C.; Capacchione, C.; Saviello, D.; Proto, A. Mechanistic Studies on Conjugated Diene Polymerizations Promoted by a Titanium Complex Containing a Tetradentate [OSSO]-Type Bis(phenolato) Ligand. *Macromolecules* **2012**, *45*, 6363−6370. (h) Buonerba, A.; Fienga, M.; Milione, S.; Cuomo, C.; Grassi, A.; Proto, A.; Capacchione, C. Binary Copolymerization of p-Methylstyrene with Butadiene and Isoprene Catalyzed by Titanium Compounds Showing Different Stereoselectivity. *Macromolecules* **2013**, *46*, 8449−8457.

(12) Cohen, A.; Yeori, A.; Goldberg, I.; Kol, M. Group 4 Complexes of a New [OSSO]-Type Dianionic Ligand. Coordination Chemistry and Preliminary Polymerization Catalysis Studies. *Inorg. Chem.* **2007**, *46*, 8114−8116.

(13) (a) Ishii, A.; Toda, T.; Nakata, N.; Matsuo, T. Zirconium Complex of an [OSSO]-Type Diphenolate Ligand Bearingtrans-1,2-Cyclooctanediylbis(thio) Core: Synthesis, Structure, and Isospecific 1-Hexene Polymerization. *J. Am. Chem. Soc.* **2009**, *131*, 13566−13567. (b) Ishii, A.; Asajima, K.; Toda, T.; Nakata, N. Synthesis of Titanium(IV) and Zirconium(IV) Complexes with an [OSSO]-Type Bis(phenolate) Ligand Bearing atrans-Cyclohexane-1,2-diyl Ring and 1-Hexene Polymerization. *Organometallics* **2011**, *30*, 2947−2956. (c) Nakata, N.; Toda, T.; Matsuo, T.; Ishii, A. Titanium Complexes Supported by an [OSSO]-Type Bis(phenolato) Ligand Based on a trans-Cyclooctanediyl Platform: Synthesis, Structures, and 1-Hexene Polymerization. *Inorg. Chem.* **2012**, *51*, 274−281. (d) Nakata, N.; Toda, T.; Matsuo, T.; Ishii, A. Controlled Isospecific Polymerization of α-Olefins by Hafnium Complex Incorporating with a trans-Cyclooctanediyl-Bridged [OSSO]-Type Bis(phenolate) Ligand. *Macromolecules* **2013**, *46*, 6758−6764. (e) Ishii, A.; Ikuma, K.; Nakata, N.; Nakamura, K.; Kuribayashi, H.; Takaoki, K. Zirconium and Hafnium Complexes with Cycloheptane- or Cyclononane-Fused [OSSO]-Type Bis(phenolato) Ligands: Synthesis, Structure, and Highly Active 1-Hexene Polymerization and Ring-Size Effects of Fused Cycloalkanes on the Activity. *Organometallics* **2017**, *36*, 3954−3966.

(14) Lapenta, R.; Buonerba, A.; De Nisi, A.; Monari, M.; Grassi, A.; Milione, S.; Capacchione, C. Stereorigid OSSO-Type Group 4 Metal Complexes in the Ring-Opening Polymerization of rac-Lactide. *Inorg. Chem.* **2017**, *56*, 3447−3458.

(15) Cohen, A.; Goldberg, I.; Venditto, V.; Kol, M. Oscillating Non-Metallocenes - from Stereoblock-Isotactic Polypropylene to Isotactic Polypropylene via Zirconium and Hafnium Dithiodiphenolate Catalysts. *Eur. J. Inorg. Chem.* **2011**, 5219−5223.

(16) Konkol, M.; Nabika, M.; Kohno, T.; Hino, T.; Miyatake, T. Synthesis, structure and α-olefin polymerization activity of group 4 metal complexes with [OSSO]-type bis(phenolate) ligands. *J. Organomet. Chem.* **2011**, *696*, 1792−1802.

(17) (a) Carvill, A.; Zetta, L.; Zannoni, G.; Sacchi, M. C. ansa-Zirconocene-Catalyzed Solution Polymerization of Propene: Influence of Polymerization Conditions on the Unsaturated Chain-End Groups. *Macromolecules* **1998**, *31*, 3783−3789. (b) Resconi, L.; Cavallo, L.; Fait, A.; Piemontesi, F. Selectivity in Propene Polymerization with Metallocene Catalysts. *Chem. Rev.* **2000**, *100*, 1253−1346.

(18) Mella, M.; Izzo, L.; Capacchione, C. Role of the Metal Center in the Ethylene Polymerization Promoted by Group 4 Complexes Supported by a Tetradentate [OSSO]-Type Bis(phenolato) Ligand. *ACS Catal.* **2011**, *1*, 1460−1468.

(19) Capacchione, C.; Proto, A.; Okuda, J. Synthesis of Branched Polyethylene by Ethylene Homopolymerization Using Titanium

DOI: 10.1021/acsomega.8b01550
ACS Omega 2018, 3, 11608−11616

Catalysts that Contain a Bridged Bis(phenolate) Ligand. *J. Polym. Sci., Part A: Polym. Chem.* **2004**, *42*, 2815−2822.
(20) Frisch, M. J.; Trucks, G. W.; Schlegel, H. B.; Scuseria, G. E.; Robb, M. A.; Cheeseman, J. R.; Scalmani, G.; Barone, V.; Mennucci, B.; Petersson, G. A.; Nakatsuji, H.; Caricato, M.; Li, X.; Hratchian, H. P.; Izmaylov, A. F.; Bloino, J.; Zheng, G.; Sonnenberg, J. L.; Hada, M.; Ehara, M.; Toyota, K.; Fukuda, R.; Hasegawa, J.; Ishida, M.; Nakajima, T.; Honda, Y.; Kitao, O.; Nakai, H.; Vreven, T.; Montgomery, J. A., Jr.; Peralta, J. E.; Ogliaro, F.; Bearpark, M.; Heyd, J. J.; Brothers, E.; Kudin, K. N.; Staroverov, V. N.; Kobayashi, R.; Normand, J.; Raghavachari, K.; Rendell, A.; Burant, J. C.; Iyengar, S. S.; Tomasi, J.; Cossi, M.; Rega, N.; Millam, J. M.; Klene, M.; Knox, J. E.; Cross, J. B.; Bakken, V.; Adamo, C.; Jaramillo, J.; Gomperts, R.; Stratmann, R. E.; Yazyev, O.; Austin, A. J.; Cammi, R.; Pomelli, C.; Ochterski, J. W.; Martin, R. L.; Morokuma, K.; Zakrzewski, V. G.; Voth, G. A.; Salvador, P.; Dannenberg, J. J.; Dapprich, S.; Daniels, A. D.; Farkas, O.; Foresman, J. B.; Ortiz, J. V.; Cioslowski, J.; Fox, D. J. *Gaussian 09*, Revision A.02; Gaussian, Inc.: Wallingford, CT, 2009.
(21) (a) Becke, A. D. Density-Functional Exchange-Energy Approximation with Correct Asymptotic Behavior. *Phys. Rev. A: At., Mol., Opt. Phys.* **1988**, *38*, 3098−3100. (b) Perdew, J. P. Density-Functional Approximation for the Correlation Energy of the Inhomogeneous Electron Gas. *Phys. Rev. B: Condens. Matter Mater. Phys.* **1986**, *33*, 8822−8824. (c) Perdew, J. P. Erratum: Density-Functional Approximation for the Correlation Energy of the Inhomogeneous Electron Gas. *Phys. Rev. B: Condens. Matter Mater. Phys.* **1986**, *34*, 7406.
(22) Hay, P. J.; Wadt, W. R. Ab initio effective core potentials for molecular calculations. Potentials for the transition metal atoms Sc to Hg. *J. Chem. Phys.* **1985**, *82*, 270−283.
(23) Schäfer, A.; Horn, H.; Ahlrichs, R. Fully Optimized Contracted Gaussian Basis Sets for Atoms Li to Kr. *J. Chem. Phys.* **1992**, *97*, 2571−2577.
(24) Legault, C. Y. *CYLview*, v1.0b; Université de Sherbrooke, 2009. http://www.cylview.org.

DOI: 10.1021/acsomega.8b01550
ACS Omega 2018, 3, 11608−11616